Article

Preparation of Mixed Bis-N-Heterocyclic Carbene Rhodium(I) Complexes

Ramón Azpíroz [1,*], Mert Olgun Karataş [1,2], Vincenzo Passarelli [1], Ismail Özdemir [2], Jesús J. Pérez-Torrente [1] and Ricardo Castarlenas [1,*]

[1] Departamento de Química Inorgánica—Instituto de Síntesis Química y Catálisis Homogénea (ISQCH), Universidad de Zaragoza—CSIC, C/Pedro Cerbuna 12, 50009 Zaragoza, Spain

[2] Department of Chemistry, Faculty of Sciences, Inonu University, 44280 Malatya, Turkey

[*] Correspondence: rayazp@unizar.es (R.A.); rcastar@unizar.es (R.C.)

Abstract: A series of mixed bis-NHC rhodium(I) complexes of type RhCl(η^2-olefin)(NHC)(NHC′) have been synthesized by a stepwise reaction of [Rh(μ-Cl)(η^2-olefin)$_2$]$_2$ with two different NHCs (NHC = N-heterocyclic carbene), in which the steric hindrance of both NHC ligands and the η^2-olefin is critical. Similarly, new mixed coumarin-functionalized bis-NHC rhodium complexes have been prepared by a reaction of mono NHC complexes of type RhCl(NHC-coumarin)(η^2,η^2-cod) with the corresponding azolium salt in the presence of an external base. Both synthetic procedures proceed selectively and allow the preparation of mixed bis-NHC rhodium complexes in good yields.

Keywords: N-heterocyclic carbene; coumarin; rhodium; mixed-NHC; anagostic interactions

1. Introduction

Since the pioneering work of Öfele [1] and Wanzlick [2] on the preparation of N-heterocyclic carbene (NHC) complexes and, particularly, that of Arduengo on the isolation of the first free NHC [3], the interest around these species in organometallic catalysis and beyond has grown exponentially [4–8]. The relatively easy synthesis enables fine tuning of their electronic and steric properties [9], which nowadays places them as the ligand of choice in many transition metal-mediated applications. Moreover, the introduction of a second carbene molecule in bis-NHC complexes have resulted in a synergic enhancement of the benefits imparted by these ligands in inter alia catalytic applications [10], the activation of small molecules [11], biomedicine [12] or luminescence [13]. Although less common, the presence of two different NHC moieties provides complementary reactivity to complexes bearing identical NHC ligands. The synthesis of these mixed bis-NHC species is not trivial due to competitive substitution reactions or the formation of isoleptic bis-NHC byproducts. To circumvent these problems, pre-synthesized unsymmetrical precursors have been used for the preparation of chelated or pincer heteroleptic bis-NHC derivatives [14–19] (Scheme 1a). Another approach involves additional functionalization after the pre-synthesis of symmetrical complexes, either within the bis-NHC backbone for multitopic ligands [20–22] (Scheme 1b), or on the wingtip of a monodentated NHC [23–25] (Scheme 1c). On the other hand, mixed monodentate bis-NHC derivatives with a variety of metals have been prepared by using a stepwise methodology [26–45] (Scheme 1d). The dissimilar stereoelectronic properties of both carbenes, such as in expanded-ring NHCs [37], mesoionic (MIC) [38–40] or acyclic carbenes [41–43], make the control of selectivity more accessible. Moreover, alternative synthetic protocols such as microwave irradiation [44] or mechanochemistry [45] have also proven to be effective.
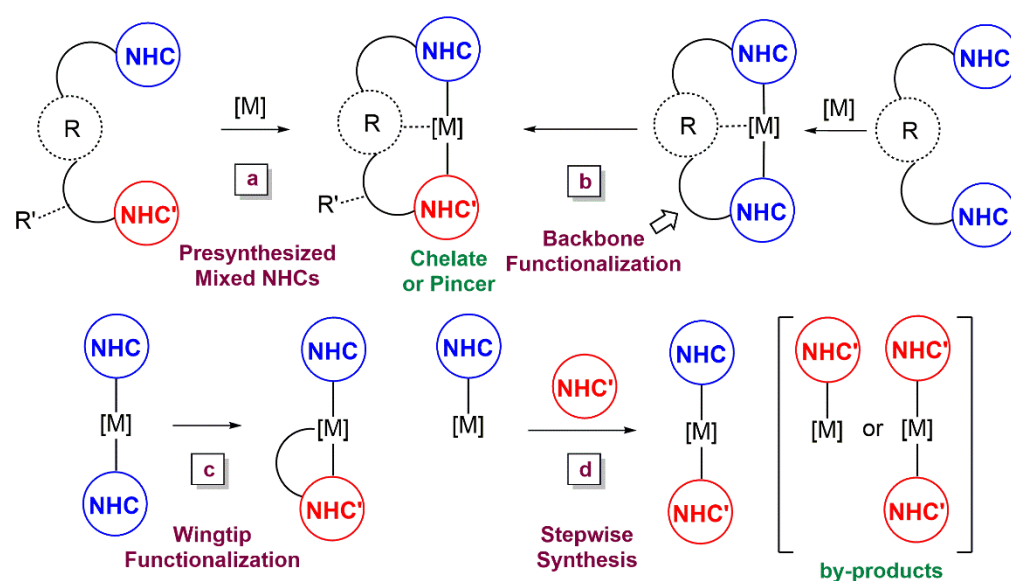
Scheme 1. Conventional synthetic approaches to mixed bis-NHC metal complexes.

Heteroleptic bis-NHC complexes have in some cases overcome the performances of isoleptic bis-NHC counterparts in many applications. For example, various mixed bis-NHC iridium [34], platinum [35], gold [36], or silver [45] complexes present promising activity as anticancer therapeutics. In material science, polystyrene-linked bis-NHC copper(I) complexes have shown application as sensors [46], whereas cyclometalated iridium (III) derivatives containing mixed NHC-acyclic carbene are top-performing emitters in organic light-emitting diodes (OLEDs) [42]. Regarding organometallic catalysis, the most relevant examples are developed for ruthenium-promoted olefin metathesis [28,41], but also for epoxide isomerization [17], hydrogen borrowing transformations [18], cross-coupling reactions [30], olefin hydrogenation [31], or azide–alkyne cycloadditions [32]. It is interesting to note the application of mixed bis-NHC palladium complexes for a reliable determination of the electronic properties of newly synthesized NHC via ^{13}C NMR spectroscopy, coined as the Huynh's Electronic Parameter (HEP) [47].

Mixed monodentate bis-NHC rhodium(I) complexes are quite scarce [26,27]. They have been prepared from dinuclear Rh-NHC precursors by CO- or chlorido-bridge cleavage with different NHC' moieties, being the marked difference in the stereoelectronic properties of both carbenes the key for success. In this context, our research group has focused on the development of rhodium-NHC complexes and their applications in catalytic processes [48–52]. In particular, the dinuclear compounds [Rh(μ-Cl)(NHC)(η^2-olefin)]$_2$ are useful starting materials for the preparation of a great variety of mononuclear complexes of type RhCl(NHC)(η^2-olefin)(L) by simple bridge-cleavage with a nucleophilic ligand, which have proven to be efficient catalysts for *gem*-selective alkyne dimerization [48,51], hydrothiolation [50], or hydropyridonation [52]. We envisaged that nitrogen-centered nucleophiles could be substituted by carbon-centered NHCs, giving access to mixed bis-NHC species. Alternatively, we have synthesized a series of imidazolium salts functionalized with a pendant coumarin group, that have allowed for the synthesis of coumarin-functionalized NHC rhodium complexes by reaction with the internal base in the dinuclear precursor [Rh(μ-OCH$_3$)(η^2,η^2-cod)]$_2$ (cod = 1,5-cyclooctadiene) [53]. In the course of our investigation, we observed that in the presence of an external base, pentacoordinated bis-coumarin-NHC rhodium derivatives were obtained. Thus, we reasoned that a stepwise reaction using different azolium salt precursors could pave the way to mixed bis-coumarin-functionalized NHC complexes.

2. Results and Discussion

The James's dimer [Rh(μ-Cl)(η^2-coe)(IPr)]$_2$ {coe = cyclooctene, IPr = 1,3-bis(2,6-diisopropylphenyl)imidazolin-2-carbene} (**1a**) [54] is a suitable precursor for the stepwise synthesis of mixed bis-NHC rhodium(I) complexes. However, initial attempts to introduce a carbene displaying stereoelectronic properties similar to IPr, such as IMes {IMes = 1,3-bis(1,3,5-trimethylphenyl)imidazolin-2-carbene}, were unsuccessful. The addition of free IMes to a C$_6$D$_6$ solution of **1a** at room temperature resulted in a complex mixture of products, including Rh-hydride species [23], in which traces of the substitution derivative [Rh(μ-Cl)(η^2-coe)(IMes)]$_2$ could be detected (Scheme 2). It is likely that the high steric hindrance imparted by both bulky NHCs, in addition to the pseudo-spherical coe ligand, could hamper the formation of the putative mixed-NHC species RhCl(η^2-coe)(IMes)(IPr). However, the steric relief imparted by the less encumbering ethylene ligand compared to coe [55], allowed the Tilset's group to prepare the bis-IMes compound RhCl(η^2-ethylene)(IMes)$_2$ [56]. Accordingly, the related IPr derivative RhCl(η^2-ethylene)(IPr)$_2$ (**2**) can now be prepared. As described previously by James et al. [54], the dinuclear Rh-IPr-coe precursor **1a** does not react with an excess of free IPr, but **2** is cleanly formed by the reaction of [Rh(μ-Cl)(η^2-ethylene)(IPr)]$_2$ (**1b**) [57] with one equivalent of free IPr under an ethylene atmosphere.
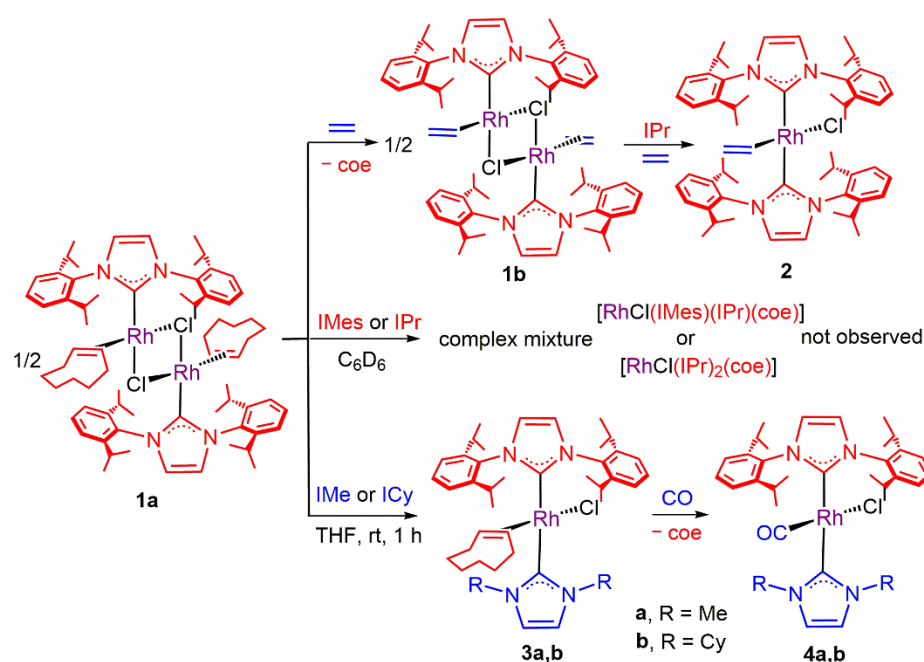

Scheme 2. Steric relief as a key factor for the preparation of bis-NHC rhodium(I) complexes.

The NMR data of **2** agree with the presence of two carbene ligands in a mutual trans disposition. In the ^{1}H NMR spectrum, the characteristic signals of IPr integrate in a double ratio with respect to that of ethylene, which appears as a singlet at δ 2.01 ppm in agreement with the C$_{2v}$ symmetry of the complex. The appearance of two septuplets at 3.51 and 2.76 ppm, corresponding to the CH-isopropyl protons of the IPr, indicates a restricted rotation of the carbene ligands around the Rh-C axis [49]. In the ^{13}C{^{1}H}-APT spectrum, the most significant feature is the downfield shift of the carbene carbon atom to δ 191.8 ppm related to **1b** (179.7 ppm), reflecting the increase of electron density at the metal center as a result of the coordination of a second powerful electron releasing IPr ligand [58]. Moreover, the reduction of the rhodium-carbon coupling (J_{Rh-C} = 41.6 Hz vs. 62.3 Hz in **1b**) is a consequence of an opposite disposition of two ligands with a strong trans influence.

The steric pressure over the η^2-olefin within a rhodium-bis-IPr architecture has been harnessed previously by Crudden et al., who described its facile decoordination un-

der a nitrogen atmosphere to yield dinitrogen adducts [59]. Unfortunately, the mixed bis-NHC derivative RhCl(η^2-ethylene)(IMes)(IPr) could not be cleanly obtained by the addition of IMes to **1b**. In addition, attempts to use diolefin precursors of the type RhCl(η^2,η^2-cod)(NHC) failed [60]. More recently, the group of Chaplin has disclosed that bis-NHC rhodium complexes bearing a η^2-coe ligand could be prepared with a less sterically demanding IBiox carbene [61]. According to this, the treatment of **1a** with less-bulky NHCs, such as IMe or ICy, prepared in situ by deprotonation of the corresponding azolium salts, resulted in the successful formation of the mixed bis-NHC complexes RhCl(η^2-coe)(IPr)(NHC) (**3**) {NHC = 1,3-dimethylimidazolin-2-carbene (IMe) (**3a**) and 1,3-dicyclohexylimidazolin-2-carbene (ICy) (**3b**)}, which were isolated as yellow solids in good yields (Scheme 2). The η^2-olefin ligand of complexes **3** remains coordinated in solution at room temperature, but can be smoothly replaced by CO to yield the carbonyl complexes RhCl(CO)(IPr)(NHC) (NHC = IMe, **4a**; ICy, **4b**). Single crystals of **3a** suitable for X-ray structure determination were grown by slow diffusion of hexane into a saturated toluene solution of the complex. Figure 1 shows the molecular structure of **3a** and the selected bond lengths and angles.
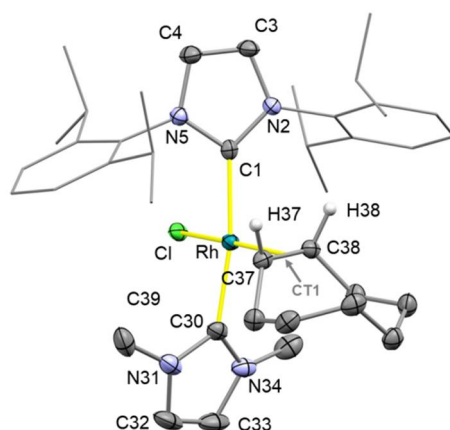

Figure 1. ORTEP view of **3a**. For clarity, most hydrogen atoms are omitted and selected groups are shown in a wireframe style. Thermal ellipsoids are at 50% probability. Selected bond lengths (Å) and angles (°) are: Rh-C1 2.061(2), Rh-C30 2.030(2), Rh-Cl 2.4215(6), Rh-CT1 2.0050(2), C37-C38 1.405(3), C1-Rh-C30 169.65(9), C30-Rh-Cl 82.13(7), C1-Rh-Cl 89.07(6), CT1-Rh-Cl 169.320(18). CT1, centroid of C37 and C38. IPr: pitch angle (θ) 5.1, yaw angle (ψ) 4.1; Ime: pitch angle (θ) 9.3, yaw angle (ψ) 2.1.

The crystal structure of **3a** shows a distorted square planar geometry at the metal center, with a trans disposition of the NHC ligands [C1-Rh-C30 169.65(9)°]. The Rh-C$_{NHC}$ bond lengths {2.061(2) Å for IPr and 2.030(2) Å for IMe} are slightly longer than that found in similar mono-NHC Rh^I-Cl-coe complexes {1.956(2) Å in [Rh(μ-Cl)(η^2-coe)(IPr)]$_2$ [60], 1.986(4) Å in RhCl(η^2-coe)(IPr)(pyridine) [57], and 1.9835(18) Å in RhCl(η^2-coe)(IPr)(2-pyridylaceton itrile) [49]}, reflecting the high trans influence of NHCs. The coordinated olefinic bond C37-C38, as well as the NHC cores of the IPr and IMe ligands, lie almost perpendicular to the coordination plane Rh-Cl-C1-C30-CT1 (79.6°, 85.3°, 69.6°, respectively). In addition, the pitch and yaw angles observed for each NHC ligand indicate a moderately distorted coordination to the metal center with respect to the corresponding rhodium-carbon bond.

The low temperature NMR data for complexes **3** agree with the structure reported in the solid state for **3a**. Thus, in the ^{1}H NMR spectrum at 243 K, two septuplets ascribed to the CH-isopropyl protons of the IPr are observed around δ 4.3 and 2.7 ppm, which broaden at room temperature due to a Rh-IPr rotational process (see Figure S1 in Supporting Information). The presence of different NHC ligands in **3** is confirmed by the appearance of two resonances for the =CHN heterocyclic protons around δ 6.5 (IPr), 5.93 (IMe, **3a**), and 6.34 ppm (ICy, **3b**). In addition, two relatively deshielded doublets are displayed in the ^{13}C{^{1}H}-APT spectrum around δ 194 (IPr), 191.4 (IMe, **3a**), and 188.0 (ICy, **3b**),

with relatively short couplings of around 42 Hz, as commented for **2**. The presence of η^2-olefin ligands is corroborated by a multiplet around δ 3 ppm in the ^{1}H NMR, and a doublet around 54 ppm (J_{C-Rh} = 16 Hz) in the ^{13}C{^{1}H}-APT spectra. The substitution of coe by carbon monoxide in **4** results in the appearance of a new doublet in the ^{13}C{^{1}H}-APT spectrum. Resonance assignment is facilitated by ^{1}H-^{13}C HMBC correlation peaks between the imidazolinyl protons and the corresponding carbene-carbon atoms within NHC moieties (Figure 2). As expected, the activation barrier for IPr-Rh rotation is reduced for carbonyl complexes **4** [49]. Therefore, only one septuplet for CH-isopropyl protons is observed around δ 3.4 ppm.
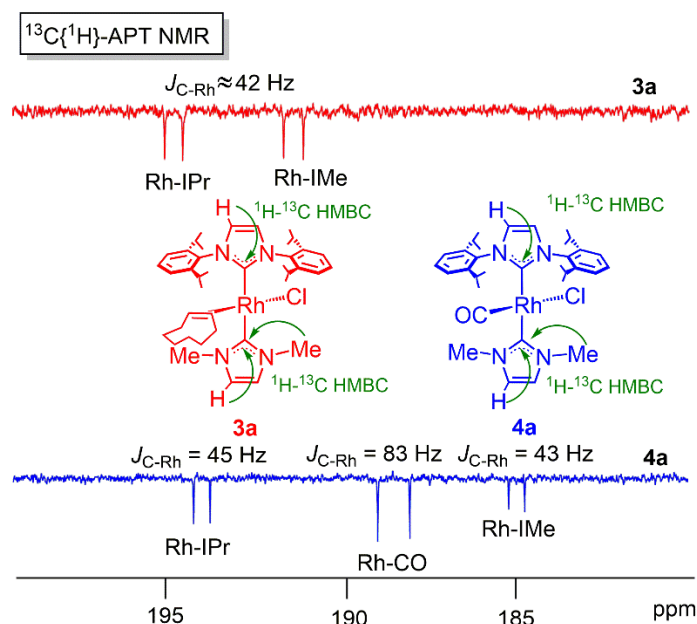

Figure 2. Downfield area of the ^{13}C{^{1}H}-APT NMR spectra of **3a** and **4a**.

Wingtip functionalized NHCs ligands can also participate in the formation of mixed bis-NHC rhodium(I) complexes. In this context, coumarin-functionalized-NHC metal complexes display interesting catalytic and luminescence properties [62–66]. In particular, we have prepared coumarin-NHC derivatives of type RhCl(NHC-Cou)(η^2,η^2-cod) (**5**) in which, in contrast to the behavior observed for related IPr- or IMes-cod compounds, the diolefin ligand can be replaced in the presence of an excess of carbene to yield bis-NHC complexes [53]. Thus, a stepwise reaction using different carbene precursors enabled the synthesis of mixed-NHC species (Scheme 3). In this way, an imidazole-benzimidazole mixed-NHC complex RhCl(κC,η^2-BzICou^{tol})(κC,η^2-ICou^{Bz}) {BzICou^{tol} = 1-(4-methylbenzyl)-3-(7,8-dimethyl-2*H*-chromen-2-one-4-yl)benzimidazolin-2-carbene, ICou^{Bz} = 1-(benzyl)-3-(7,8-dimethyl-2*H*-chromen-2-one-4-yl)imidazolin-2-carbene} (**6**) was obtained by refluxing a THF solution of the precursor RhCl(BzICou^{tol})(η^2,η^2-cod) (**5a**) and the azolium salt [HICou^{Bz}]Cl in the presence of sodium methoxide for 24 h. Under similar reaction conditions, RhCl(BzICou^{Bu})(IPr) (**7**) was formed starting from RhCl(BzICou^{bu})(η^2,η^2-cod) (**5b**) and free IPr. Although the solid state structure of **6** could not be determined by X-ray diffraction methods, a trigonal bipyramidal structure with a trans disposition of the NHC ligands is assumed in an analogy to the related coumarin-functionalized bis-NHC complexes RhCl(BzICou^R)$_2$ and RhCl(ICou^R)$_2$ described previously [53]. Interestingly, the X-ray single-crystal analysis of the mixed bis-NHC compound **7** revealed a cis disposition for the IPr and coumarin-BzI carbenes, an uncommon feature in square planar rhodium(I) complexes when a trans configuration is feasible [67,68] (Figure 3).
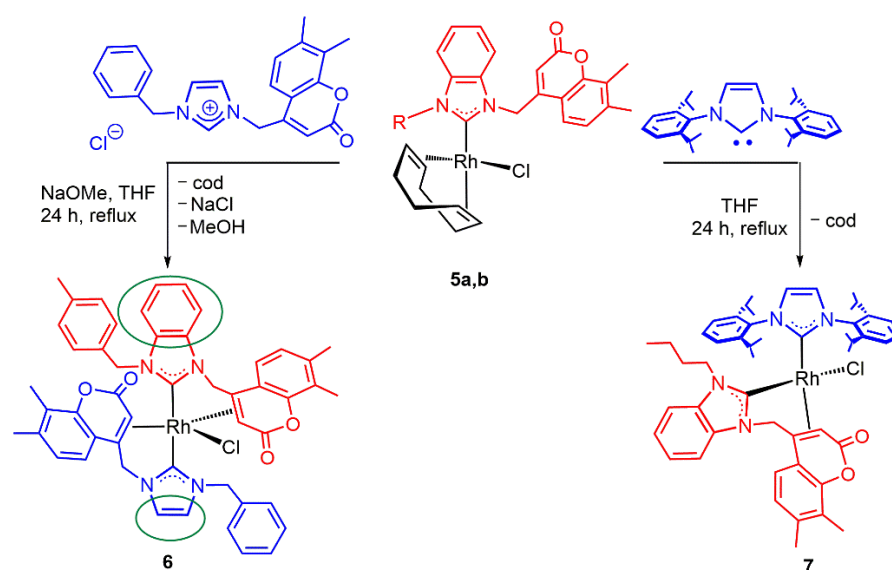
Scheme 3. Preparation of coumarin-functionalized mixed bis-NHC rhodium complexes.
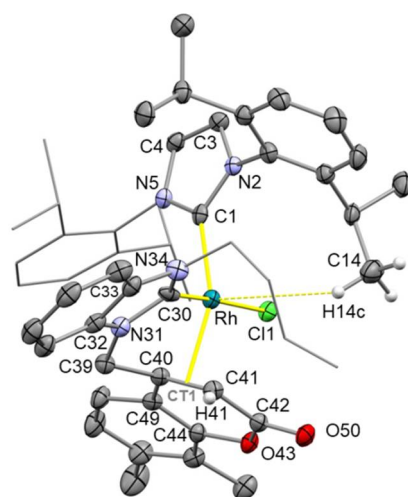

Figure 3. ORTEP view of **7**. For clarity, most hydrogen atoms are omitted and selected groups are shown in a wireframe style. Thermal ellipsoids are at 50% probability. Selected bond lengths (Å) and angles (°) are: Rh-Cl1 2.4116(8), Rh-C1 2.070(3), Rh-C30 1.959(3), Rh-CT1 2.0294(3), C40-C41 1.428(4), C30-Rh-C1 98.57(12), C1-Rh-Cl1 85.11(8), C30-Rh-Cl1 175.78(9), CT1-Rh-Cl1 97.55(2), CT1-Rh-C1 153.84(9), C30-Rh-CT01 80.07(9). IPr: pitch angle (θ) 12.7, yaw angle (ψ) 3.4; BzICou^{Bu}: pitch angle (θ) 0.5, yaw angle (ψ) 11.1. CH···Rh contact: Rh·H14c 3.06(4), C14-H14c 0.90(4), Rh·C 3.774(4), Rh-H14c-C14 138(3).

The crystal structure of **7** exhibits a severely distorted square planar coordination geometry at the metal center with an Rh·H-C short contact. In fact, the NHC moieties adopt a cis disposition [C30-Rh-C1 98.57(12)°] with the chlorido ligand lying trans to C30 from the BzICou^{Bu} ligand [C30-Rh-Cl1 175.78(9)°]. On the other hand, the angle CT1-Rh-C1 [153.84(9)°] between C1 from the IPr ligand and the centroid of the coordinated olefinic bond C40-C41 of the coumarin moiety is significantly smaller than the ideal value for a trans disposition. In addition, the short Rh···H14c-C14 [3.06(4) Å] contact is observed [r_{vdW}(H) + r_{vdw}(Rh) ≈ 3.2 Å] [69], possibly indicating the presence of an anagostic interaction between one IPr methyl group and the metal center [70]. The Rh-C$_{NHC}$ distances are quite different {1.959(3) Å for BzI-Cou vs. 2.070(3) Å for IPr}, likely as a consequence of the higher trans influence of the olefin related to chlorido ligand. As for the bidentate BzICou^{Bu} ligand, its reduced bite angle [80.07(9)°] brings about a severe deviation of the

NHC core from the ideal arrangement with respect to the Rh-C30 bond (yaw angle, ψ 11.1°), similar to what is already observed in the related bis-chelate complexes RhCl(BzICou^R)$_2$ and RhCl(ICou^R)$_2$ [71].

The presence of two different NHC ligands in **6** and **7** is confirmed by the NMR data. The ^{13}C{^{1}H}-APT NMR spectrum of **6** display two doublets at δ 184.8 and 172.4 ppm with Rh-C coupling constants around 33 Hz, ascribed to carbene carbon atoms. Correlations of the imidazolinyl protons at δ 6.45 and 6.40 ppm with the carbon signal at 172.4 ppm in the ^{1}H-^{13}C-HMBC spectrum of **6** helps to ascribe that signal to the I-Cou ligand (Figure 4). In addition, four doublets with J_{H-H}~13 Hz are observed for the N-methylene protons in the ^{1}H NMR spectrum. The coordination of the olefinic group of coumarin moieties is reflected in the appearance of high field doublets at 72.0 ppm (J_{C-Rh} = 12.1 Hz) and 50.8 ppm (J_{C-Rh} = 7.2 Hz) for BzI-Cou and 74.0 ppm (J_{C-Rh} = 11.7 Hz) and 52.5 ppm (J_{C-Rh} = 7.6 Hz) ascribed to the I-Cou ligand. Regarding 7, the presence of two different NHC ligands is corroborated by the observation of two low field doublets at 196.1 ppm (J_{C-Rh} = 52.2 Hz) and 191.1 ppm (J_{C-Rh} = 60.2 Hz) for BzI-Cou and IPr, respectively, in the ^{13}C{^{1}H}-APT NMR spectrum. The deshielding of these resonances compared to those of **6** could be ascribed to a more electron-rich rhodium center due to the coordination of only one electron-acceptor olefin ligand, whereas the higher J_{C-Rh} values reflect Rh-C shorter separations.
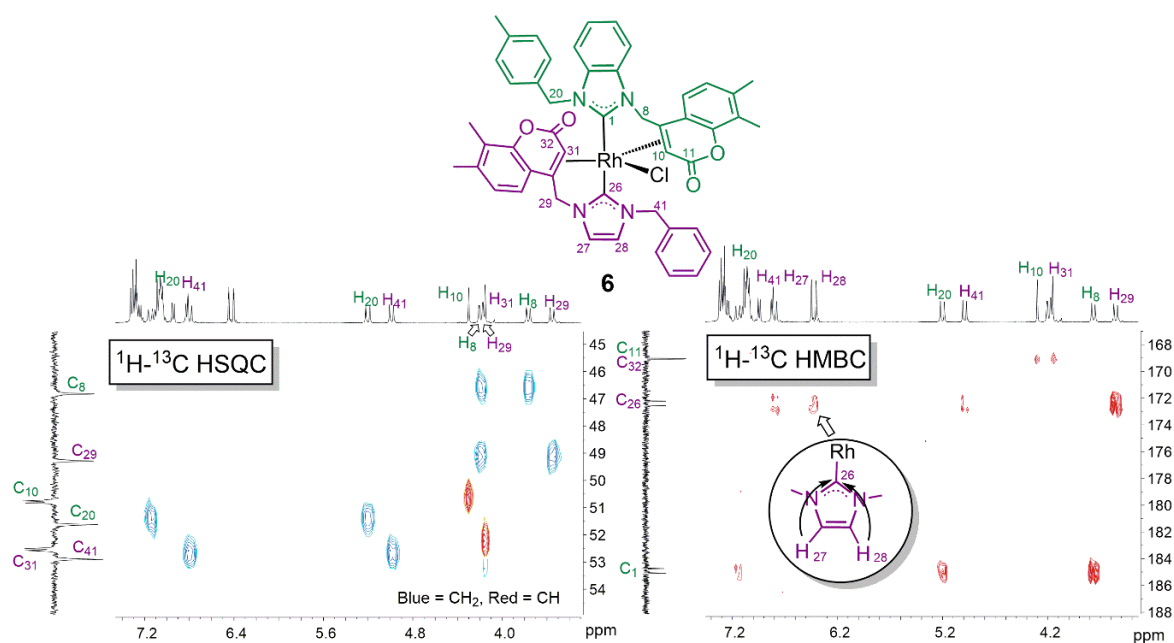
Figure 4. Selected areas of 2D-NMR correlation spectra for **6**: ^{1}H-^{13}C HSQC (**left**) and ^{1}H-^{13}C HMBC (**right**).

3. Materials and Methods

All reactions were carried out with the rigorous exclusion of air and moisture, using Schlenk-tube techniques and a dry box when necessary. The reagents were purchased from commercial suppliers and used as received. Organic solvents were dried by standard procedures and distilled under argon prior to use, or obtained oxygen- and water-free from a Solvent Purification System (Innovative Technologies). Deuterated solvents were deoxygenated and dried over sodium metal (C$_6$D$_6$ and toluene-d_8) or activated molecular sieves (CDCl$_3$). The organometallic precursors [Rh(μ-Cl)(η^2-coe)(IPr)]$_2$ (**1a**) [54], [Rh(μ-Cl)(η^2-ethylene)(IPr)]$_2$ (**1b**) [57], and RhCl(η^2,η^2-cod)(NHC-Cou) (**5**) [53] were prepared as previously described in the literature. Chemical shifts (expressed in parts per million) are referenced to residual solvent peaks. Coupling constants, *J*, are given in Hz. Spectral assignments were achieved by a combination of ^{1}H-^{1}H COSY, ^{13}C{^{1}H}-APT and ^{1}H-^{13}C HSQC/HMBC experiments. The attenuated total reflection infrared spectra

(ATR-IR) of solid samples were run on a PerkinElmer Spectrum 100 FT-IR spectrometer. C, H, and N analyses were carried out in a Perkin–Elmer 2400 CHNS/O analyzer. High-resolution electrospray mass spectra (HRMS) were acquired using a MicroTOF-Q hybrid quadrupole time-of-flight spectrometer (Bruker Daltonics, Bremen, Germany).

Preparation of RhCl(η^2-CH$_2$=CH$_2$)(IPr)$_2$ (2). A solution of complex **1b** (300 mg, 0.27 mmol) and free IPr (230 mg, 0.59 mmol) in 50 mL of toluene was treated with 2 bars of ethylene and stirred for 1 h at room temperature. After filtration through Celite, the solvent was evaporated to dryness. The addition of n-hexane induced the precipitation of a yellow solid, which was washed with n-hexane (3 × 4 mL) and dried in vacuo. Yield (392 mg, 77%). HRMS (ESI) *m/z* Calcd for RhC$_{54}$H$_{72}$N$_4$ (M-C$_2$H$_4$-Cl): 879.4807. Found: 879.4840. ^{1}H NMR (400.1 MHz, C$_6$D$_6$, 298 K): δ 7.28 (t, J_{H-H} = 7.9, 4H, H$_{p-IPr}$), 7.20 and 7.06 (both d, J_{H-H} = 7.9, 8H, H$_{m-IPr}$), 6.34 (s, 4H, =CHN), 3.51 and 2.76 (both sept, J_{H-H} = 7.1, 8H, C$\underline{H}$Me$_{IPr}$), 2.01 (d, J_{H-Rh} = 2.0, 4H, CH$_2$=CH$_2$), 1.27, 1.08, 0.98, and 0.96 (all d, J_{H-H} = 7.1, 48H, CHM$\underline{e}$$_{IPr}$). ^{13}C{^{1}H}-APT NMR (75.5 MHz, C$_6$D$_6$, 298 K): δ 191.8 (d, J_{C-Rh} = 41.6, Rh-C$_{IPr}$), 148.4 and 145.2 (both s, C$_{q-IPr}$), 138.2 (s, C$_q$N), 129.1 (s, CH$_{p-IPr}$), 124.3 and 123.0 (both s, CH$_{m-IPr}$), 123.9 (s, =CHN), 38.8 (d, J_{C-Rh} = 15.7, CH$_2$=CH$_2$), 28.8 and 28.5 (both s, $\underline{C}$HMe$_{IPr}$), 26.3, 26.2, 23.2, and 22.9 (all s, CHM$\underline{e}$$_{IPr}$). Figure S2: 1H NMR spectrum of 2 in C6D6 at 298 K. Figure S3. 13C{1H}-APT NMR spectrum of 2 in C6D6 at 298 K. Figure S4. 1H-1H COSY NMR spectrum of 2 in C6D6 at 298 K. Figure S5. 1H-13C HSQC NMR spectrum of 2 in C6D6 at 298 K. Figure S6. 1H-13C HMBC NMR spectrum of 2 in C6D6 at 298 K.

Preparation of RhCl(η^2-coe)(IMe)(IPr) (3a). A solution of dinuclear complex **1a** (300 mg, 0.23 mmol) in 50 mL of toluene was treated with a solution of IMe (50 mg, 0.51 mmoles) in THF and stirred for 1h at room temperature. After filtration through Celite, the solvent was evaporated to dryness. The addition of n-hexane induced the precipitation of a yellow solid, which was washed with n-hexane (3 × 4 mL) and dried in vacuo. Yield: 280 mg (83%). Anal. Calcd. for C$_{40}$H$_{58}$N$_4$ClRh: C, 65.52; H, 7.97; N, 7.64. Found: C, 65.63; H, 7.99; N, 7.62. ^{1}H NMR (300.1 MHz, toluene-d_8, 243 K): δ 7.4-7.2 (6H, H$_{Ph-IPr}$), 6.63 (s, 2H, =CHN$_{IPr}$), 5.93 (s, 2H, =CHN$_{IMe}$), 4.41 and 2.58 (both sept, J_{H-H} = 6.6, 4H, C$\underline{H}$Me$_{IPr}$), 3.46 (s, 6H, Me$_{IMe}$), 2.97 (m, 2H, =CH$_{coe}$), 1.8-0.8 (12H, coe), 1.66, 1.42, 1.14, and 1.01 (all d, J_{H-H} = 6.6, 24H, CHM$\underline{e}$$_{IPr}$). ^{13}C{^{1}H}-APT NMR (75.5 MHz, toluene-d_8, 243 K): δ 194.9 (d, J_{C-Rh} = 41.2, Rh-C$_{IPr}$), 191.4 (d, J_{C-Rh} = 43.8, Rh-C$_{IMe}$), 148.5 and 146.3 (both s, C$_{q-IPr}$), 137.8 (s, C$_q$N), 129.3 (s, CH$_{p-IPr}$), 124.3 and 122.4 (both s, CH$_{m-IPr}$), 123.7 (s, =CHN$_{IPr}$), 120.2 (s, =CHN$_{IMe}$), 54.1 (d, J_{C-Rh} = 16.8, =CH$_{coe}$), 37.2 (s, Me$_{IMe}$), 28.9 and 28.7 (both s, $\underline{C}$HMe$_{IPr}$), 31.7, 30.9, and 26.8 (all s, CH$_{2-coe}$), 27.0, 26.8, 23.2, and 22.4 (all s, CHM$\underline{e}$$_{IPr}$). Figure S7. 1H NMR spectrum of 3a in toluene-d8 at 243 K. Figure S8. 13C{1H}-APT NMR spectrum of 3a in toluene-d8 at 243 K. Figure S9. 1H-1H COSY NMR spectrum of 3a in toluene-d8 at 243 K. Figure S10. 1H-13C HSQC NMR spectrum of 3a in toluene-d8 at 243 K. Figure S11. 1H-13C HSQC NMR spectrum of 3a in toluene-d8 at 243 K.

Preparation of RhCl)(η^2-coe)(ICy)(IPr) (3b) A solution of dinuclear complex **1a** (300 mg, 0.23 mmol) in 50 mL of toluene was treated with a solution of ICy (118 mg, 0.51 mmoles) in THF and stirred for 1h at room temperature. After filtration through Celite, the solvent was evaporated to dryness. The addition of n-hexane induced the precipitation of a yellow solid, which was washed with n-hexane (3 × 4 mL) and dried in vacuo. Yield: 387 mg (87%). Anal. Calcd. for C$_{50}$H$_{74}$N$_4$ClRh: C, 69.07; H, 8.58; N, 6.44. Found: C, 68.83; H, 8.61; N, 6.62. ^{1}H NMR (300.1 MHz, toluene-d_8, 243 K): δ 7.4-7.2 (6H, H$_{Ph-IPr}$), 6.52 (s, 2H, =CHN$_{IPr}$), 6.34 (s, 2H, =CHN$_{ICy}$), 5.10 (t, J_{H-H} = 10.1, 2H, CH$_{cy}$), 4.15 and 2.70 (both sept, J_{H-H} = 6.1, 4H, C$\underline{H}$Me$_{IPr}$), 3.11 (m, 2H, =CH$_{coe}$), 2.9-0.8 (32H, CH$_2$), 1.66, 1.48, 1.12, and 1.00 (all d, J_{H-H} = 6.1, 24H, CHM$\underline{e}$$_{IPr}$). ^{13}C{^{1}H}-APT NMR (75.5 MHz, toluene-d_8, 243 K): δ 192.8 (d, J_{C-Rh} = 41.2, Rh-C$_{IPr}$), 188.0 (d, J_{C-Rh} = 45.5, Rh-C$_{ICy}$), 148.0 and 146.0 (both s, C$_{q-IPr}$), 138.2 (s, C$_q$N), 129.2 (s, CH$_{p-IPr}$), 124.9 and 122.5 (both s, CH$_{m-IPr}$), 124.1 (s, =CHN$_{IPr}$), 126.1 (s, =CHN$_{ICy}$), 57.8 (s, CH$_{cy}$), 54.5 (d, J_{C-Rh} = 16.4, =CH$_{coe}$), 35.0, 33.4, 32.6, 30.8, 25.9, and 25.7 (all s, CH$_2$), 28.8 and 28.7 (both s, $\underline{C}$HMe$_{IPr}$), 26.8, 26.7, 24.0, and 22.5 (all s, CHM$\underline{e}$$_{IPr}$). Figure S12. 1H NMR spectrum of 3b in toluene-d8 at 243 K. Figure S13. 13C{1H}-APT NMR

spectrum of 3b in toluene-d8 at 243 K. Figure S14. 1H-1H COSY NMR spectrum of 3b in toluene-d8 at 243 K. Figure S15. 1H-13C HSQC NMR spectrum of 3b in toluene-d8 at 243 K. Figure S16. 1H-13C HMBC NMR spectrum of 3b in toluene-d8 at 243 K.

Preparation of RhCl(CO)(IMe)(IPr) (4a). Carbon monoxide was bubbled through a yellow solution of **3a** (100 mg, 0.14 mmol) in 20 mL of toluene at room temperature for 30 min. After filtration through Celite, the solvent was evaporated to dryness. The addition of n-hexane induced the precipitation of a yellow solid, which was washed with n-hexane (3×4 mL) and dried in vacuo. Yield: 66 mg (71%). IR (cm^{-1}, pure sample): 1935 ν(CO). HRMS (ESI) m/z Calcd for $RhC_{33}H_{44}N_4O$ (M-Cl): 615.2565. Found: 615.2568. ^1H NMR (400.1 MHz, C_6D_6, 298 K): δ 7.46 (m, 2H, H_{p-IPr}), 7.39 (m, 4H, H_{m-IPr}), 6.90 (s, 2H, =CHN_{IPr}), 5.91 (s, 2H, =CHN_{IMe}), 3.59 (sept, J_{H-H} = 6.8, 4H, $C\underline{H}Me_{IPr}$), 3.30 (s, 6H, Me_{IMe}), 1.71 and 1.26 (both d, J_{H-H} = 6.8, 24H, $CH\underline{Me}_{IPr}$). $^{13}C\{^1H\}$-APT NMR (100.4 MHz, C_6D_6, 298 K): δ 193.2 (d, J_{C-Rh} = 44.7, Rh-C_{IPr}), 188.5 (d, J_{C-Rh} = 83.0, CO), 185.3 (d, J_{C-Rh} = 42.7, Rh-C_{IMe}), 147.0 (s, C_{q-IPr}), 137.3 (s, C_qN), 129.4 (s, CH_{p-IPr}), 123.6 (s, =CHN_{IPr}), 123.5 (s, CH_{m-IPr}), 120.4 (s, =CHN_{IMe}), 37.2 (s, Me_{IMe}), 28.9 (s, $\underline{C}HMe_{IPr}$), 26.3 and 22.9 (both s, $CH\underline{Me}_{IPr}$). Figure S17. 1H NMR spectrum of 4a in C6D6 at 298 K. Figure S18. 13C{1H}-APT NMR spectrum of 4a in C6D6 at 298 K. Figure S19. 1H-1H COSY NMR spectrum of 4a in C6D6 at 298 K. Figure S20. 1H-13C HSQC NMR spectrum of 4a in C6D6 at 298 K. Figure S21. 1H-13C HMBC NMR spectrum of 4a in C6D6 at 298 K.

Preparation of RhCl(CO)(ICy)(IPr) (4b). Carbon monoxide was bubbled through a yellow solution of **3b** (100 mg, 0.13 mmol) in 20 mL of toluene at room temperature for 30 min. After filtration through Celite, the solvent was evaporated to dryness. The addition of n-hexane induced the precipitation of a yellow solid, which was washed with n-hexane (3×4 mL) and dried in vacuo. Yield (76 mg, 83%). IR (cm^{-1}, pure sample): 1937 ν(CO). HRMS (ESI) m/z Calcd for $RhC_{43}H_{60}N_4O$ (M-Cl): 751.3817. Found: 751.3795. ^1H NMR (400.1 MHz, toluene-d_8, 243 K): δ 7.32 (m, 2H, H_{p-IPr}), 7.24 (m, 4H, H_{m-IPr}), 6.76 (s, 2H, =CHN_{IPr}), 6.34 (s, 2H, =CHN_{ICy}), 4.84 (m, 2H, CH_{cy}), 3.38 (sept, J_{H-H} = 6.5, 4H, $C\underline{H}Me_{IPr}$), 2.0–0.8 (all m, 20H, CH_2), 1.52 and 1.13 (both d, J_{H-H} = 6.5, 24H, $CH\underline{Me}_{IPr}$). $^{13}C\{^1H\}$-APT NMR (100.4 MHz, toluene-d_8, 243 K): δ 193.8 (d, J_{C-Rh} = 41.6, Rh-C_{IPr}), 188.6 (d, J_{C-Rh} = 81.4, CO), 183.6 (d, J_{C-Rh} = 40.6, Rh-C_{ICy}), 147.3 (s, C_{q-IPr}), 137.7 (s, C_qN), 129.5 (s, CH_{p-IPr}), 123.9 (s, CH_{m-IPr}), 123.8 (s, =CHN_{IPr}), 116.2 (s, =CHN_{ICy}), 59.4 (s, CH_{cy}), 33.9, 33.4, 25.8, 25.7, and 25.5 (all s, CH_2), 28.9 (s, $\underline{C}HMe_{IPr}$), 26.5 and 23.1 (both s, $CH\underline{Me}_{IPr}$). Figure S22. 1H NMR spectrum of 4b in toluene-d8 at 243 K. Figure S23. 13C{1H}-APT NMR spectrum of 4b in toluene-d8 at 243 K. Figure S24. 1H-1H COSY NMR spectrum of 4b in toluene-d8 at 243 K. Figure S25. 1H-13C HSQC NMR spectrum of 4b in toluene-d8 at 243 K. Figure S26. 1H-13C HMBC NMR spectrum of 4b in toluene-d8 at 243 K.

Preparation of RhCl($\kappa C,\eta^2$-BzICou^{tol})($\kappa C,\eta^2$-ICou^{Bz}) (6). (Figure 5) A mixture of RhCl(BzICou^{tol})(η^2,η^2-cod) (**5a**) (100 mg, 0.15 mmol), the imidazolium precursor [HICou^{Bz}]Cl (60 mg, 0.15 mmol) and NaOCH$_3$ (8 mg, 0.15 mmol) in 20 mL of THF was heated under reflux for 24 h. After this period, the mixture was cooled to 0 °C which resulted in the formation of a precipitate. The mother liquor was removed and the solid washed with cold THF (2×5 mL). Then, the solid was dissolved in 20 mL of CH_2Cl_2 and filtered through Celite. The solution was concentrated to ca. 1 mL, and then n-hexane was added to induce the precipitation of a white solid which was washed with n-hexane (3×5 mL) and dried in vacuo. Yield: 30 mg (45%). HRMS (ESI) m/z Calcd for $RhC_{49}H_{44}N_4O_4$ (M-Cl): 855.2412. Found: 855.2427. ^1H NMR (400.1 MHz, $CDCl_3$, 253 K): δ 7.68 (d, J_{H-H} = 8.0, 1H, H_{16}), 7.54 (d, J_{H-H} = 7.9, 1H, H_{37}), 7.53 (d, J_{H-H} = 7.8, 2H, H_{43}), 7.30 (dd, J_{H-H} = 7.8, 7.4, 2H, H_{44}), 7.29–7.22 (3H, $H_{22,45}$), 7.14 and 5.20 (both d, J_{H-H} = 14.8, 2H, H_{20}), 7.10–7.03 (6H, $H_{4,5,6,15,23}$), 6.94 (both d, J_{H-H} = 7.7, 1H, H_{36}), 6.82 (d, J_{H-H} = 7.2, 1H, H_3), 6.79 and 4.99 (both d, J_{H-H} = 13.8, 2H, H_{41}), 6.45 (d, J_{H-H} = 1.7, 1H, H_{27}), 6.40 (d, J_{H-H} = 1.7, 1H, H_{28}), 4.30 (br, 1H, H_{10}), 4.19 and 3.55 (both d, J_{H-H} = 13.2, 2H, H_{29}), 4.19 and 3.76 (both d, J_{H-H} = 13.2, 2H, H_8), 4.15 (br, 1H, H_{31}), 2.24 (s, 3H, H_{19}), 2.23 (s, 3H, H_{25}), 2.10 (s, 3H, H_{18}), 1.80 (s, 3H, H_{40}), 1.34 (s, 3H, H_{39}). $^{13}C\{^1H\}$-APT NMR (100.4 MHz, $CDCl_3$, 253 K): δ 184.8 (d, J_{C-Rh} = 32.0, Rh-C_1), 172.4 (d, J_{C-Rh} = 34.4, Rh-C_{26}), 169.1 (s, O=C_{11}), 169.0 (s, O=C_{32}), 147.4 (s, C_{12}), 146.7 (s, C_{33}),

138.2 (s, C_{35}), 138.1 (s, C_{14}), 137.1 (s, C_{24}), 137.0 (s, C_{42}), 134.4 (s, C_7), 133.5 (s, C_{21}), 132.0 (s, C_2), 129.8 (s, C_{43}), 129.2 (s, C_{23}), 128.6 (s, C_{22}), 128.4 (s, C_{44}), 128.0 (s, C_{45}), 124.9 (s, C_{13}), 124.5 (s, C_{34}), 124.4 (s, C_{15}), 124.1 (s, C_{36}), 123.0 (s, C_4), 122.9 (s, C_5), 121.8 (s, C_{28}), 121.1 (s, C_{17}), 120.8 (s, C_{38}), 119.2 (s, C_{16}), 118.8 (s, C_{37}), 117.9 (s, C_{27}), 112.4 (s, C_6), 109.2 (s, C_3), 74.0 (d, $J_{C\text{-}Rh}$ = 11.7, C_{30}), 72.0 (d, $J_{C\text{-}Rh}$ = 12.1, C_9), 52.9 (s, C_{41}), 52.5 (d, $J_{C\text{-}Rh}$ = 7.6, C_{31}), 51.6 (s, C_{20}), 50.8 (d, $J_{C\text{-}Rh}$ = 7.2, C_{10}), 49.3 (s, C_{29}), 46.8 (s, C_8), 21.4 (s, C_{25}), 20.4 (s, C_{19}), 19.9 (s, C_{40}), 11.8 (s, C_{18}), 10.8 (s, C_{39}). Figure S27. 1H NMR spectrum of 6 in toluene-d8 at 253 K. Figure S28. 13C{1H}-APT NMR spectrum of 6 in toluene-d8 at 253 K. Figure S29. 1H-13C HSQC NMR spectrum of 6 in toluene-d8 at 253 K. Figure S30. 1H-13C HMBC NMR spectrum of 6 in toluene-d8 at 253 K.
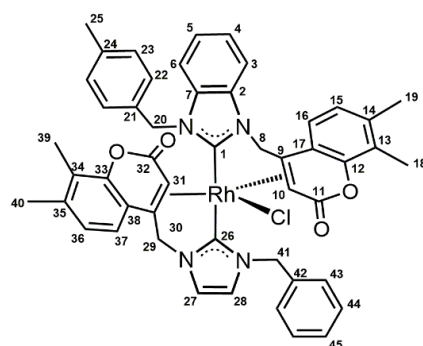
Figure 5. Numbering of atoms for complex **6**.

Preparation of RhCl(κC,η^2-BzICou^{Bu})(IPr) (7). (Figure 6) A mixture of RhCl (BzICou^{Bu})(η^2,η^2-cod) (100 mg, 0.15 mmol) (**5b**) and free IPr (70, 0.18 mmol) in 20 mL of THF was heated under reflux for 24 h. After this period, THF was removed and then n-hexane was added to induce the precipitation of a white solid which was washed with n-hexane (3 × 5 mL) and dried in vacuo. Yield: 40 mg (29%). Anal. Calcd. for $C_{50}H_{60}N_4ClO_2Rh$: C, 67.67; H, 6.81; N, 6.31. Found: C, 67.62; H, 6.79; N, 6.42. ^{1}H NMR (400.1 MHz, toluene-d_8, 253 K): δ 7.37 and 7.24 (both t, $J_{H\text{-}H}$ = 7.8, 2H, $H_{p\text{-}IPr}$), 7.18 and 7.10 (both d, $J_{H\text{-}H}$ = 7.8, 4H, $H_{m\text{-}IPr}$), 6.90 and 6.87 (both dd, $J_{H\text{-}H}$ = 7.4, 7.1, 2H, $H_{4,5}$), 6.70 and 6.64 (both d, $J_{H\text{-}H}$ = 7.5, 2H, $H_{3,6}$), 6.65 (d, $J_{H\text{-}H}$ = 8.0, 2H, H_{15}), 6.46 and 6.39 (both d, $J_{H\text{-}H}$ = 1.6, 2H, =CHN), 6.00 (d, $J_{H\text{-}H}$ = 8.0, 1H, H_{16}), 4.47, 3.26, 2.79, and 1.81 (all sept, $J_{H\text{-}H}$ = 6.7, 4H, C$\underline{H}$Me$_{IPr}$), 4.16 and 2.41 (both d, $J_{H\text{-}H}$ = 13.4, 2H, H_8), 3.07 and 2.65 (both m, 2H, H_{20}), 2.32 (s, 3H, H_{18}), 2.20 (br, 1H, H_{10}), 2.09 (s, 3H, H_{19}), 1.35 and 1.28 (both m, 4H, $H_{21,22}$), 1.01 (t, $J_{H\text{-}H}$ = 7.3, 3H, H_{23}), 1.74, 1.06, 0.95, 0.90, 0.87, 0.80, 0.53, and 0.53 (all d, $J_{H\text{-}H}$ = 6.7, 24H, CHM$\underline{e}_{IPr}$). ^{13}C{^{1}H}-APT NMR (100.4 MHz, toluene-d_8, 253 K): δ 196.1 (d, $J_{C\text{-}Rh}$ = 52.2, Rh-C_{BzICou}), 191.1 (d, $J_{C\text{-}Rh}$ = 60.8, Rh-C_{IPr}), 168.4 (s, O=C_{11}), 150.6 (s, C_{12}), 148.9, 146.9, 146.4, and 142.4 (all s, $C_{q\text{-}IPr}$), 138.6 and 137.0 (both s, C_qN), 136.5 (s, C_{17}), 134.8 and 134.4 (both s, $C_{2,7}$), 130.1 and 129.1 (both s, $C_{p\text{-}IPr}$), 129.0, 128.4, 127.5, and 126.2 (all s, $C_{m\text{-}IPr}$), 125.0 and 124.6 (both s, =CHN), 124.7 (s, C_{15}), 124.2 (s, C_{13}), 122.9 (s, C_{14}), 122.1 and 121.7 (both s, $C_{4,5}$), 121.4 (s, C_{16}), 109.4 and 109.2 (both s, $C_{3,6}$), 73.6 (d, $J_{C\text{-}Rh}$ = 17.9, C_9), 50.1, (s, C_8), 46.2 (s, C_{20}), 39.8 (d, $J_{C\text{-}Rh}$ = 7.0, C_{10}), 32.6 and 30.4 (both s, $C_{21,22}$), 28.6, 28.2, 28.1, and 27.9 (all s, C$\underline{H}$Me$_{IPr}$), 26.9, 26.4, 25.8, 25.7, 25.6, 23.0, 22.8, and 20.4 (all s, CHM$\underline{e}_{IPr}$), 20.3 (s, C_{19}), 14.2 (s, C_{23}), 12.3 (s, C_{18}). Figure S31. 1H NMR spectrum of 7 in toluene-d8 at 253 K. Figure S32. 13C{1H}-APT NMR spectrum of 7 in toluene-d8 at 253 K. Figure S33. 1H-13C HSQC NMR spectrum of 7 in toluene-d8 at 253 K. Figure S34. 1H-13C HMBC NMR spectrum of 7 in toluene-d8 at 253 K.

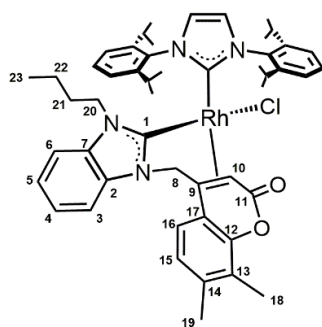**Figure 6.** Numbering of atoms for complex **7**.

Crystal Structure Determination: Single crystals of **3a** and **7** for the X-ray diffraction studies were grown by slow diffusion of hexane into a saturated toluene solution (**3a**) or slow evaporation of CDCl$_3$ solution in a NMR tube (**7**). X-ray diffraction data were collected at 100(2) K on a Bruker APEX DUO CCD diffractometer with graphite-monochromated Mo−Kα radiation ($\lambda = 0.71073$ Å) using ω rotations. The intensities were integrated and corrected for absorption effects with SAINT–PLUS [72] and SADABS [73] programs, both included in the APEX2 package. The structures were solved by the Patterson method with SHELXS-97 [74] and refined by full matrix least-squares on F^2 with SHELXL-2014 [71], under WinGX [75]. CCDC 2204568 (**3a**) and 2204569 (**7**) contain the supplementary crystallographic data for this paper. These data can be obtained free of charge via http://www.ccdc.cam.ac.uk/conts/retrieving.html, accessed on 17 October 2022 (or from the CCDC, 12 Union Road, Cambridge CB2 1EZ, UK; Fax: +44-12-2333-6033; E-mail: deposit@ccdc.cam.ac.uk).

Crystal data and structure refinement for 3a. C$_{40}$H$_{58}$ClN$_4$Rh, 733.26 g·mol^{-1}, monoclinic, $P2_1/n$, $a = 11.2372(5)$ Å, $b = 17.7258(7)$ Å, $c = 19.8602(8)$ Å, $\beta = 104.6600(10)°$, $V = 3827.1(3)$ Å^3, $Z = 4$, $D_{calc} = 1.273$ g·cm^{-3}, $\mu = 0.548$ mm^{-1}, $F(000) = 1552$, yellow prism, $0.160 \times 0.080 \times 0.050$ mm^3, $\theta_{min}/\theta_{max}$ 1.563/26.022°, index ranges $-13 \leq h \leq 13$, $-21 \leq k \leq 21$, $-24 \leq l \leq 24$, reflections collected/independent 46716/7524 [R(int) = 0.0509], T_{min}/T_{max} 0.9486/0.8307, data/restraints/parameters 7524/0/425, GooF(F^2) = 1.015, $R_1 = 0.0319$ [I > 2σ(I)], $wR_2 = 0.0744$ (all data), largest diff. peak/hole 1.098/−0.473 e·Å^{-3}.

Crystal data and structure refinement for 7. C$_{50}$H$_{60}$ClN$_4$O$_2$Rh·2.5 CH$_2$Cl$_2$, 1099.69 g·mol^{-1}, monoclinic, $P2_1/n$, $a = 14.1094(12)$ Å, $b = 20.7235(18)$ Å, $c = 18.0797(16)$ Å, $\beta = 96.0110(10)°$, $V = 5257.4(8)$ Å^3, $Z = 4$, $D_{calc} = 1.389$ g·cm^{-3}, $\mu = 0.673$ mm^{-1}, $F(000) = 2284$, red prism, $0.170 \times 0.160 \times 0.145$ mm^3, $\theta_{min}/\theta_{max}$ 1.965/26.372°, $-17 \leq h \leq 17$, $-25 \leq k \leq 25$, $-22 \leq l \leq 22$, reflections collected/independent 91967/10757 [R(int) = 0.0514], T_{min}/T_{max} 0.8596/0.7205, data/restraints/parameters 10757/15/636, GooF(F^2) = 1.118, $R_1 = 0.0445$ [I > 2σ(I)], $wR_2 = 0.1104$ (all data), largest diff. peak/hole 0.720/−1.106 e·Å^{-3}.

4. Conclusions

Mixed bis-NHC rhodium(I) complexes of type RhCl(η^2-olefin)(NHC)(NHC′) have been synthesized following a stepwise procedure. It has been revealed that the steric hindrance imparted by the wingtips of the carbene ligands as well as that of the η^2-olefin is critical. Thus, bis-NHC derivatives containing both bulky IPr or IMes could be accessed only for smaller η^2-ethylene, whereas the steric relief in IMe or ICy allows for the preparation of mixed bis-NHC complexes containing a η^2-coe ligand. Regarding the use of RhCl(NHC)(η^2,η^2-cod) precursors, in contrast to the stability observed for IPr derivative, the coumarin-functionalized NHC ligands facilitates decoordination of the diolefin, enabling the straightforward introduction of a second NHC. Thus, the pentacoordinated mixed bis-NHC complexes bearing coumarin functionalities adopt a trans-NHC disposition, whereas the square planar IPr-BzIcou species presents an uncommon cis-NHC configuration, exhibiting an anagostic interaction between the metal atom and one IPr methyl group.

References

1. Öfele, K. 1,3-Dimethyl-4-imidazolinyliden-(2)-pentacarbonylchrom ein neuer übergangsmetall-carben-komplex. *J. Organomet. Chem.* **1968**, *12*, P42–P43. [CrossRef]
2. Wanzlick, H.-W.; Schönherr, H.-J. Direct synthesis of a mercury salt-carbene complex. *Angew. Chem. Int. Ed.* **1968**, *7*, 141–142. [CrossRef]
3. Arduengo, A.J., III; Harlow, R.L.; Kline, M.A. Stable crystalline carbene. *J. Am. Chem. Soc.* **1991**, *113*, 361–363. [CrossRef]
4. Herrmann, W.A. N-Heterocyclic carbenes: A new concept in organometallic catalysis. *Angew. Chem. Int. Ed.* **2002**, *41*, 1290–1309. [CrossRef]
5. Visbal, R.; Gimeno, M.C. N-heterocyclic carbene metal complexes: Photoluminescence and applications. *Chem. Soc. Rev.* **2014**, *43*, 3551–3574. [CrossRef]
6. Smith, C.A.; Narouz, M.R.; Lummis, P.A.; Singh, I.; Nazemi, A.; Li, C.-H.; Crudden, C.M. N-Heterocyclic carbenes in materials chemistry. *Chem. Rev.* **2018**, *119*, 4986–5056. [CrossRef]
7. Ott, I. Metal N-heterocyclic carbene complexes in medicinal chemistry. *Adv. Inorg. Chem.* **2020**, *75*, 121–148. [CrossRef]

8.   Bellotti, P.; Koy, M.; Hopkinson, M.N.; Glorius, F. Recent advances in the chemistry and applications of N-heterocyclic carbenes. *Nat. Chem. Rev.* **2021**, *5*, 711–725. [CrossRef]

9.   Benhamou, L.; Chardon, E.; Lavigne, G.; Bellemin-Laponnaz, S.; César, V. Synthetic routes to N-heterocyclic carbene precursors. *Chem. Rev.* **2011**, *111*, 2705–2733. [CrossRef]

10. Gardinier, M.G.; Ho, C.C. Recent advances in bidentate bis(N-heterocyclic carbene) transition metal complexes and their applications in metal-mediated reactions. *Coord. Chem. Rev.* **2018**, *375*, 373–388. [CrossRef]

11. Yamashita, M.; Goto, K.; Kawashima, T. Fixation of both O_2 and CO_2 from air by a crystalline palladium complex bearing N-heterocyclic carbene ligands. *J. Am. Chem. Soc.* **2005**, *127*, 7294–7295. [CrossRef] [PubMed]

12. Hickey, J.L.; Ruhayel, R.A.; Barnard, P.J.; Murray, V.; Baker, M.V.; Berners-Price, S.J.; Filipovska, A. Mitochondria-targeted chemotherapeutics: The rational design of Gold(I) *N*-heterocyclic carbene complexes that are selectively toxic to cancer cells and target protein selenols in preference to thiols. *J. Am. Chem. Soc.* **2008**, *130*, 12570–12571. [CrossRef] [PubMed]

13. Henwood, A.F.; Lesieur, M.; Bansal, A.K.; Lemaur, V.; Beljonne, D.; Thompson, D.G.; Graham, D.; Slawin, A.M.Z.; Samuel, I.D.W.; Cazin, C.S.J.; et al. Palladium(0) NHC complexes: A new avenue to highly efficient phosphorescence. *Chem. Sci.* **2015**, *6*, 3248–3261. [CrossRef] [PubMed]

14. Viciano, M.; Feliz, M.; Corberán, R.; Mata, J.A.; Clot, E.; Peris, E. Aliphatic versus aromatic C-H activation in the formation of abnormal carbenes with iridium: A combined experimental and theoretical study. *Organometallics* **2007**, *26*, 5304–5314. [CrossRef]

15. Gardiner, M.G.; Ho, C.C.; Mackay, F.M.; McGuinness, D.S.; Tucker, M. Selective and adaptable access to N,N′-asymmetrically substituted imidazol-2-ylidene bis-NHC ligands: Pd(II) complexes featuring wide variation in N-alkyl and aryl steric bulk. *Dalton Trans.* **2013**, *42*, 7447–7457. [CrossRef]

16. Aznarez, F.; Sanz Miguel, P.J.; Tan, T.T.Y.; Hahn, F.E. Preparation of rhodium(III) di-NHC chelate complexes featuring two different NHC donors via a mild NaOAc-assisted C−H activation. *Organometallics* **2016**, *35*, 410–419. [CrossRef]

17. Tian, Y.; Jürgens, E.; Mill, K.; Jordan, R.; Maulbetsch, T.; Kunz, D. Nucleophilic isomerization of epoxides by pincer-rhodium catalysts: Activity increase and mechanistic insights. *ChemCatChem* **2019**, *11*, 4028–4035. [CrossRef]

18. Donthireddy, S.N.R.; Illam, P.M.; Rit, A. Ruthenium(II) complexes of heteroditopic N-heterocyclic carbene ligands: Efficient catalysts for C−N bond formation via a hydrogen-borrowing strategy under solvent-free conditions. *Inorg. Chem.* **2020**, *59*, 1835–1847. [CrossRef]

19. Danopoulos, A.A.; Tsoureas, N.; Wright, J.A.; Light, M.E. N-Heterocyclic pincer dicarbene complexes of iron(II): C-2 and C-5 metalated carbenes on the same metal center. *Organometallic* **2004**, *23*, 166–168. [CrossRef]

20. Zuo, W.; Braunstein, P. N-Heterocyclic dicarbene iridium(III) pincer complexes featuring mixed NHC/abnormal NHC ligands and their applications in the transfer dehydrogenation of cyclooctane. *Organometallics* **2012**, *31*, 2606–2615. [CrossRef]

21. Hermosilla, P.; García-Orduña, P.; Sanz Miguel, P.J.; Polo, V.; Casado, M.A. Nucleophilic reactivity at a =CH arm of a lutidine-based CNC/Rh system: Unusual alkyne and CO_2 activation. *Inorg. Chem.* **2022**, *61*, 7120–7129. [CrossRef] [PubMed]

22. Dorta, R.; Stevens, E.D.; Nolan, S.P. Double C-H activation in a Rh-NHC complex leading to the isolation of a 14-electron Rh(III) complex. *J. Am. Chem. Soc.* **2004**, *126*, 5054–5055. [CrossRef] [PubMed]

23. Tang, C.Y.; Smith, W.; Vidovic, D.; Thompson, A.L.; Chaplin, A.B.; Aldridge, S. Sterically encumbered iridium Bis(N-heterocyclic carbene) systems: Multiple C-H activation processes and isomeric normal/abnormal carbene complexes. *Organometallics* **2009**, *28*, 3059–3063. [CrossRef]

24. Zenkina, O.V.; Keske, E.C.; Wang, R.; Crudden, C.M. Double single-crystal-to-single-crystal transformation and small-molecule activation in rhodium NHC complexes. *Angew. Chem. Int. Ed.* **2011**, *50*, 8100–8104. [CrossRef]

25. Clement, N.D.; Cavell, K.J.; Jones, C.; Elsevier, C.J. Oxidative addition of imidazolium salts to Ni0 and Pd0: Synthesis and structural characterization of unusually stable metal–hydride complexes. *Angew. Chem. Int. Ed.* **2004**, *43*, 1277–1279. [CrossRef]

26. Burling, S.; Douglas, S.; Mahon, M.F.; Nama, D.; Pregosin, P.; Whittlesey, M.K. Cationic tris N-heterocyclic carbene rhodium carbonyl complexes: Molecular structures and solution NMR studies. *Organometallics* **2006**, *25*, 2642–2648. [CrossRef]

27. Bittermann, A.; Herdtweck, E.; Härter, P.; Herrmann, W.A. Rhodium(I), a carbene-transfer transition-metal ion and a synthetic route to symmetrical and asymmetrical substituted trans-RhCl(CO)(NHC)(NHC) complexes. *Organometallics* **2009**, *28*, 6963–6968. [CrossRef]

28. Sashuk, V.; Peeck, L.H.; Plenio, H. [(NHC)NHCewg)RuCl$_2$(CHPh)] complexes with modified NHCewg ligands for efficient Ring-Closing Metathesis leading to tetrasubstituted olefins. *Chem. Eur. J.* **2010**, *16*, 3983–3993. [CrossRef]

29. Gaillard, S.; Nun, P.; Slawin, A.M.Z.; Nolan, S.P. Expeditious synthesis of [Au(NHC)(L)](NHC = N-Heterocyclic Carbene; L = Phosphine or NHC) Complexes. *Organometallics* **2010**, *29*, 5402–5408. [CrossRef]

30. Liu, Z.-H.; Xu, Y.-C.; Xie, L.-Z.; Sun, H.-M.; Shen, Q.; Zhang, Y. Controlled synthesis of nickel(II) dihalides bearing two different or identical N-heterocyclic carbene ligands and the influence of carbene ligands on their structures and catalysis. *Dalton Trans.* **2011**, *40*, 4697–4706. [CrossRef]

31. Lund, C.L.; Sgro, M.J.; Cariou, R.; Stephan, D.W. A cis-bis-mixed-carbene ruthenium hydride complex: An olefin-selective hydrogenation catalyst. *Organometallics* **2012**, *31*, 802–805. [CrossRef]

32. Lazreg, F.; Slawin, A.M.Z.; Cazin, C.S.J. Heteroleptic bis(N-heterocyclic carbene)copper(I) complexes: Highly efficient systems for the [3+2] cycloaddition of azides and alkynes. *Organometallics* **2012**, *31*, 7969–7975. [CrossRef]

33. César, V.; Barthes, C.; Farré, Y.C.; Cuisiat, S.V.; Vacher, B.Y.; Brousses, R.; Lugan, N.; Lavigne, G. Anionic and zwitterionic copper(I) complexes incorporating an anionic N-heterocyclic carbene decorated with a malonate backbone: Synthesis, structure and catalytic applications. *Dalton Trans.* **2013**, *42*, 7373–7385. [CrossRef]

34. Gothe, Y.; Marzo, T.; Messori, L.; Metzler-Nolte, N. Iridium(I) compounds as prospective anticancer agents: Solution chemistry, antiproliferative profiles and protein interactions for a series of iridium(I) N-heterocyclic carbene complexes. *Chem. Eur. J.* **2016**, *22*, 12487–12494. [CrossRef] [PubMed]

35. Rehm, T.; Rothemund, M.; Muenzner, J.K.; Noor, A.; Kempeb, R.; Schobert, R. Novel cis-[(NHC)₁(NHC)₂(L)Cl]platinum(II) complexes–synthesis, structures, and anticancer activities. *Dalton Trans.* **2016**, *45*, 15390–15398. [CrossRef] [PubMed]

36. Sen, S.; Yi, L.; Lynch, M.; Arumugan, K.; He, X.-P.; Sessler, J.L.; Arambula, J.F. Expanding the biological utility of bis-NHC gold(I) complexes through post synthetic carbamate conjugation. *Chem. Commun.* **2019**, *55*, 10627–10630. [CrossRef]

37. Kumar, A.; Yuan, D.; Huynh, H.V. Stereoelectronic profiling of expanded-ring N-heterocyclic carbenes. *Inorg. Chem.* **2019**, *58*, 7545–7553. [CrossRef]

38. Lebel, H.; Janes, M.K.; Charette, A.B.; Nolan, S.P. Structure and Reactivity of "Unusual" N-Heterocyclic Carbene (NHC) Palladium Complexes Synthesized from Imidazolium Salts. *J. Am. Chem. Soc.* **2004**, *126*, 5046–5047. [CrossRef]

39. Appelhans, L.N.; Incarvito, C.D.; Crabtree, R.H. Synthesis of monodentate bis(N-heterocyclic carbene) complexes of iridium: Mixed complexes of abnormal NHCs, normal NHCs, and triazole NHCs. *J. Organomet. Chem.* **2008**, *693*, 2761–2766. [CrossRef]

40. Mejuto, C.; Guisado-Barrios, G.; Gusev, D.; Peris, E. First homoleptic MIC and heteroleptic NHC–MIC coordination cages from 1,3,5-triphenylbenzenebridged tris-MIC and tris-NHC ligands. *Chem. Commun.* **2015**, *51*, 13914–13917. [CrossRef]

41. Liberman-Martin, A.L.; Grubbs, R.H. Ruthenium olefin metathesis catalysts featuring a labile carbodicarbene ligand. *Organometallics* **2017**, *36*, 4091–4094. [CrossRef]

42. Na, H.; Cañada, L.M.; Wen, Z.; Wu, J.I.-C.; Teets, T.S. Mixed-carbene cyclometalated iridium complexes with saturated blue luminescence. *Chem. Sci.* **2019**, *10*, 6254–6260. [CrossRef] [PubMed]

43. Singh, C.; Kumar, A.; Huynh, H.V. Stereoelectronic profiling of acyclic diamino carbenes (ADCs). *Inorg. Chem.* **2020**, *59*, 8451–8460. [CrossRef] [PubMed]

44. Lazreg, F.; Cordes, D.B.; Slawin, A.M.Z.; Cazin, C.S.J. Synthesis of homoleptic and heteroleptic bis-N-heterocylic carbenegroup 11 complexes. *Organometallics* **2015**, *34*, 419–425. [CrossRef]

45. Beillard, A.; Quintin, F.; Gatignol, J.; Retailleau, P.; Renaud, J.-L.; Gaillard, S.; Métro, T.-X.; Lamaty, F.; Bantreil, X. Solving the challenging synthesis of highly cytotoxic silver complexes bearing sterically hindered NHC ligands with mechanochemistry. *Dalton Trans.* **2020**, *49*, 12592–12598. [CrossRef]

46. Biewend, M.; Neumann, S.; Michael, P.; Binder, W.H. Synthesis of polymer-linked copper(I) bis(N-heterocyclic carbene) complexes of linear and chain extended architecture. *Polym. Chem. Trans.* **2019**, *10*, 1078–1088. [CrossRef]

47. Teng, Q.; Huynh, H.V. A unified ligand electronic parameter based on ^{13}C NMR spectroscopy of N-heterocyclic carbene complexes. *Dalton Trans.* **2017**, *46*, 614–627. [CrossRef] [PubMed]

48. Azpíroz, R.; Rubio-Pérez, L.; Castarlenas, R.; Pérez-Torrente, J.J.; Oro, L.A. gem-selective cross-dimerization and cross-trimerization of alkynes with silylacetylenes promoted by a rhodium–pyridine–N-heterocyclic carbene catalyst. *ChemCatChem* **2014**, *6*, 2587–2592. [CrossRef]

49. Palacios, L.; Di Giuseppe, A.; Castarlenas, R.; Lahoz, F.J.; Pérez-Torrente, J.J.; Oro, L.A. Pyridine versus acetonitrile coordination in rhodium–N-heterocyclic carbene square-planar complexes. *Dalton Trans.* **2015**, *44*, 5777–5789. [CrossRef]

50. Palacios, L.; Meheut, Y.; Galiana-Cameo, M.; Artigas, M.J.; Di Giuseppe, A.; Lahoz, F.J.; Polo, V.; Castarlenas, R.; Pérez-Torrente, J.J.; Oro, L.A. Design of highly selective alkyne hydrothiolation Rh^{I}-NHC catalysts: Carbonyl-triggered non-oxidative mechanism. *Organometallics* **2017**, *36*, 2198–2207. [CrossRef]

51. Galiana-Cameo, M.; Urriolabeitia, A.; Barrenas, E.; Passarelli, V.; Pérez-Torrente, J.J.; Di Giuseppe, A.; Polo, V.; Castarlenas, R. Metal−Ligand cooperative proton transfer as an efficient trigger for rhodium-NHC-pyridonato catalyzed gem-specific alkyne dimerization. *ACS Catal.* **2021**, *11*, 7553–7567. [CrossRef]

52. Galiana-Cameo, M.; Romeo, R.; Urriolabeitia, A.; Passarelli, V.; Pérez-Torrente, J.J.; Polo, V.; Castarlenas, R. Rhodium-NHC-catalyzed *gem*-specific *O*-selective hydropyridonation of terminal alkynes. *Angew. Chem. Int. Ed.* **2022**, *61*, e202117006. [CrossRef] [PubMed]

53. Karataş, M.O.; Di Giuseppe, A.; Passarelli, V.; Alıcı, B.; Pérez-Torrente, J.J.; Oro, L.A.; Özdemir, I.; Castarlenas, R. Pentacoordinated rhodium(I) complexes supported by coumarin-functionalized N-heterocyclic carbene ligands. *Organometallics* **2018**, *37*, 191–202. [CrossRef]

54. Yu, X.-Y.; Patrick, B.O.; James, B.R. Rhodium(III) peroxo complexes containing carbene and phosphine ligands. *Organometallics* **2006**, *25*, 4870–4877. [CrossRef]

55. Palacios, L.; Di Giuseppe, A.; Artigas, M.J.; Polo, V.; Lahoz, F.J.; Castarlenas, R.; Pérez-Torrente, J.J.; Oro, L.A. Mechanistic insight into the pyridine enhanced α-selectivity in alkyne hydrothiolation catalysed by quinolinolate–rhodiumIJI)–N-heterocyclic carbene complexes. *Catal. Sci. Technol.* **2016**, *6*, 8548–8561. [CrossRef]

56. Fooladi, E.; Dalhus, B.; Tilset, M. Synthesis and characterization of half-sandwich N-heterocyclic carbene complexes of cobalt and rhodium. *Dalton Trans.* **2004**, *22*, 3909–3917. [CrossRef]

57. Di Giuseppe, A.; Castarlenas, R.; Pérez-Torrente, J.J.; Crucianelli, M.; Polo, V.; Sancho, R.; Lahoz, F.J.; Oro, L.A. Ligand-controlled regioselectivity in the hydrothiolation of alkynes by rhodium N-Heterocyclic carbene catalysts. *J. Am. Chem. Soc.* **2012**, *134*, 8171–8183. [CrossRef]

58. Galiana-Cameo, M.; Passarelli, V.; Perez-Torrente, J.J.; Di Giuseppe, A.; Castarlenas, R. Variation on the π-acceptor ligand within a Rh^I-N-heterocyclic carbene framework: Divergent catalytic outcomes for phenylacetylene-methanol transformations. *Eur. J. Inorg. Chem.* **2021**, *2021*, 2947–2957. [CrossRef]

59. Praetorius, J.M.; Wang, R.; Crudden, C.M. Structure and reactivity of dinitrogen rhodium complexes containing N-Heterocyclic carbene ligands. *Eur. J. Inorg. Chem.* **2009**, *2009*, 1746–1751. [CrossRef]

60. Zenkina, O.V.; Keske, E.C.; Kochhar, G.S.; Wang, R.; Crudden, C.M. Heteroleptic rhodium NHC complexes with pyridine derived ligands: Synthetic accessibility and reactivity towards oxygen. *Dalton Trans.* **2013**, *42*, 2282–2293. [CrossRef]

61. Chaplin, A.B. Rhodium(I) complexes of the conformationally rigid IBioxMe$_4$ ligand: Preparation of mono-, bis-, and tris-ligated NHC complexes. *Organometallics* **2014**, *33*, 3069–3077. [CrossRef]

62. Achar, G.; Shahini, C.R.; Patil, S.A.; Budagumpi, S. Synthesis, structural characterization, crystal structures and antibacterial potentials of coumarin-tethered N-heterocyclic carbene silver(I) complexes. *J. Organomet. Chem.* **2017**, *833*, 28–42. [CrossRef]

63. Halter, O.; Plenio, H. Fluorescent dyes in organometallic chemistry: Coumarin-tagged NHC–metal complexes. *Eur. J. Inorg. Chem.* **2018**, *25*, 2935–2943. [CrossRef]

64. Ruiz-Mendoza, F.J.; Mendoza-Espinosa, D.; Gonzalez-Montiel, S. Synthesis and catalytic activity of coumarin- and chrysin-Tethered Triazolylidene Gold(I) Complexes. *Eur. J. Inorg. Chem.* **2018**, *42*, 4622–4629. [CrossRef]

65. Karataş, M.O.; Alıcı, B.; Passarelli, V.; Özdemir, I.; Pérez-Torrente, J.J.; Castarlenas, R. Iridium(I) complexes bearing hemilabile coumarin functionalised N-heterocyclic carbene ligands with application as alkyne hydrosilylation catalysts. *Dalton Trans.* **2021**, *50*, 11206–11215. [CrossRef]

66. Akpunar, C.; Özdemir, N.; Karataş, M.O.; Alıcı, B.; Özdemir, I. Synthesis, crystal structures and catalytic activities of palladium complexes with coumarin-functionalised N-heterocyclic carbene ligands. *Inorg. Chem. Commun.* **2021**, *131*, 108755. [CrossRef]

67. Herrmann, W.A.; Frey, G.D.; Herdtweck, E.; Steinbeck, M. Synthesis and characterization of N-heterocyclic carbene substituted phosphine and phosphite rhodium Complexes and their Catalytic properties in hydrogenation reactions. *Adv. Synth. Catal.* **2007**, *349*, 1677–1691. [CrossRef]

68. Ahmida, A.; Elmagbari, F.M.; Egold, H.; Flörke, U.; Henkel, G. NHC-phosphane rhodium complexes and their reaction with oxygen. *Polyhedron* **2020**, *181*, 114472. [CrossRef]

69. Batsanov, S.S. Van der Waals Radii of Elements. *Inorg. Mater.* **2001**, *37*, 871–885. [CrossRef]

70. Brookhart, M.; Green, M.L.H.; Parkin, G. Agostic interactions in transition metal compounds. *Proc. Natl. Acad. Sci. USA* **2007**, *104*, 6908–6914. [CrossRef]

71. Sheldrick, G.M. Crystal structure refinement with SHELXL. Acta Crystallogr. *Sect. C Struct. Chem.* **2015**, *71*, 3–8. [CrossRef] [PubMed]

72. *SAINT+: Area-Detector Integration Software*, version 6.01; Bruker AXS: Madison, WI, USA, 2001.

73. Sheldrick, G.M. *SADABS Program*; University of Göttingen: Göttingen, Germany, 1999.

74. Sheldrick, G.M. *SHELXS 97, Program for the Solution of Crystal Structure*; University of Göttingen: Göttingen, Germany, 1997.

75. Farrugia, L.J. WinGX and ORTEP for Windows: An update. *J. Appl. Crystallogr.* **2012**, *45*, 849–854. [CrossRef]